Identification of MRC2 and CD209 receptors as targets for photodynamic therapy of retinoblastoma using mesoporous silica nanoparticles

A. Gallud, D. Warther, M. Maynadier, M. Sefta, F. Poyer, C.D. Thomas, C. Rouxel, O. Mongin, M. Blanchard-Desce, A. Morère, et al.

RSC Advances

ROYAL SOCIETY OF CHEMISTRY

www.rsc.org/advances

Journal Name

COMMUNICATION

Identification of MRC2 and CD209 receptors as targets for photodynamic therapy of retinoblastoma using mesoporous silica nanoparticles

Received 00th January 20xx,
Accepted 00th January 20xx

DOI: 10.1039/x0xx00000x

www.rsc.org/

A. Gallud,[a] D. Warther,[b] M. Maynadier,[c] M. Sefta,[d] F. Poyer,[e,#] C. D. Thomas, [e,#] C. Rouxel,[f] O. Mongin,[f] M. Blanchard-Desce,[f,#] A. Morère,[a] L. Raehm,[b] P. Maillard,[g,#*] J.O. Durand,[b,#*] M. Garcia,[a] and M. Gary-Bobo.[a*]

Research in nanomedicine has grown rapidly over the past few years and is playing a key role in the development of effective treatments for ophthalmological purpose. Retinoblastoma is an intraocular tumor triggered by genetic mutation in young children and photodynamic therapy (PDT) is currently developed as a promising non-mutagenic approach to treat this cancer. In this work, we have first identified two receptors, MRC2 and CD209, which are highly expressed by retinoblastoma. Then, we developed mesoporous silica nanoparticles (MSN) grafted with antibodies anti-MRC2 and/or anti-CD209 for retinoblastoma PDT and imaging.

Retinoblastoma is a malignant intraocular tumor of childhood which remains relatively unknown due to its low rarity with an incidence of 1 for 20,000 births. The role of genomic instability of the retinoblastoma gene Rb1 localized on chromosome 13q and the most relevant epidemiological issues concerning retinoblastoma have been pointed out to explain the various clinical expression of the disease [1-3]. Treatment options mainly depend on the size, the location of the tumor and the genetic form [4, 5]. In the worst advanced clinical case, when the chances to save vision are poor and the risk of dissemination is high, enucleation is realized. On the contrary, if a possibility to preserve the vision exists, conservative treatments can be applied. In this context, the development of a non-mutagen treatment such as photodynamic therapy, allowing a high selectivity, could be of particular interest.

The use of lectins for direct therapeutic targeting has drawn attention in various research areas including cancers [6-11]. In this way, glycoconjugated-porphyrins were synthesized to obtain efficient photosensitizers against retinoblastoma cells for one-photon photodynamic therapy (PDT) [12-14]. To develop more effective therapies for ophthalmological purposes, nanomedicine could play a key role. There are a number of nanomedicine tools offering innovative solutions to ophthalmological issues and targeted therapy is the clue for therapeutic efficiency improvement [15]. In our previous work, mannose or galactose functionalized-mesoporous silica nanoparticles (MSN) were designed for PDT and drug delivery for retinoblastoma treatment [16, 17]. In continuation to this work and to enhance the specific targeting of retinoblastoma, we investigated four members of the mannose receptor family which belong to the group VI of C-type lectin superfamily. Gene expression of MRC2, PLA2R, LY75 and CD209 were examined by transcriptomic analysis on 37 human retinoblastoma tumors. Then, expression levels of these receptors were investigated by immunohistochemistry and Western blot on Y-79 and WERI-Rb1 retinoblastoma cells and on tumor tissues (Rb102, Rb111 and Rb200) derived from xenografted mice models. Finally, we evaluated the targeting of retinoblastoma cells by antibodiy-grafted MSN and their therapeutic efficiency using two-photon PDT. For the study of mannose receptors as targets for retinoblastoma treatment, the expression of macrophage mannose receptor 1 (MRC1), C-type mannose receptor 2 (MRC2), lymphocyte antigen 75 (LY75), phospholipase A2 receptor (PLA2R) and CD209 receptor (see ESI, Figure S1) were analyzed.

First, a transcriptomic analysis was conducted on the gene expression of PLA2R, LY75, CD209 and MRC2 in retinoblastoma using Affymetrix U133 plus 2.0 arrays (MRC1 is not probed on these arrays). Transcriptomic profiling was thus performed on a total of 37 primary human retinoblastoma tumors (Figure 1). For PLA2R, LY75 and CD209, mean sample gene expression values were of 2.6, 2.8 and 3.5, respectively (log-scaled). The mean gene expression of MRC2 was 6.6. In addition, the analysis of the open dataset from McEvoy et al. confirms these expression profiles (see ESI, Figure S2). This is in accordance with previous obtained results in 4

[a] *Institut des Biomolécules Max Mousseron de Montpellier, UMR 5247 CNRS-Université Montpellier-ENSCM, Bâtiment (E), Faculté de Pharmacie, 15 avenue Charles Flahault BP14491, 34093 Montpellier, France. E-mail: magali.gary-bobo@inserm.fr*
[b] *Institut Charles Gerhardt Montpellier, UMR5253, CNRS-UM2-ENSCM-UM1, CC1701 Place Eugène Bataillon, 34095 Montpellier Cedex 05, France. E-mail: durand@univ-montp2.fr.fr*
[c] *NanoMedSyn, 15, avenue Charles Flahault BP14491, 34093 Montpellier, France.*
[d] *Institut Curie, UMR144, Hôpital, 26 rue d'Ulm, 75248 Paris Cedex 05, France*
[e] *Institut Curie, U759 INSERM, Bât 112, Université Paris-Sud, Centre Universitaire, F-91405 Orsay, France.*
[f] *Chimie et Photonique Moléculaires, CNRS UMR6510, Campus de Beaulieu, Université Rennes 1, 35042 Rennes Cedex, France Institut régional du Cancer Montpellier, Chirurgie A2, 208 Avenue des Apothicaires 34298 Montpellier, France.*
[g] *Institut Curie, UMR176 CNRS, Bât 112, Université Paris-Sud, Centre Universitaire, F-91405 Orsay, France. E-mail: philippe.maillard@curie.fr,*
[#] *CNRS GDR 3049 PHOTOMED, UMR5623, Université Paul Sabatier, F 31062 Toulouse*
Electronic Supplementary Information (ESI) available: [details of any supplementary information available should be included here]. See DOI: 10.1039/x0xx00000x

retinoblastoma cell lines (WERI-Rb1, Y-79, RB113 and RB355) and 55 additional primary human tumors [3]. These results highlight the significant MRC2 gene expression in retinoblastoma cell lines and tumors.

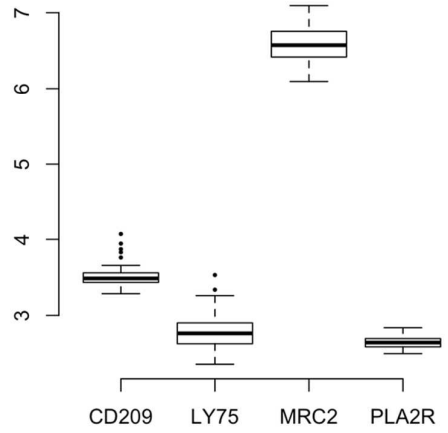

Figure 1. Box plots of normalized relative scores for CD209, LY75, MRC2 and PLA2R type-specific gene signatures for 37 retinoblastoma human tumors.

To evaluate protein expression and to confirm results obtained by transcriptomic analysis, immunohistochemistry experiments were performed on retinoblastoma cells and human tumors obtained from xenografted mouse (Figure 2A). Y-79 and WERI-Rb1 cells were fixed, permeabilized and immunostained. Anti-PLA2R, anti-LY75 [18], anti-CD209 [19, 20], anti-MRC2 [21, 22], and anti-MRC1 [23, 24] antibodies were used for immunocytochemistry experiments after a validation of their specificity in stringent processes. Anti-IgG rabbit and anti-IgG mouse antibodies were used as negative control of unspecific staining.

In Y-79 cells, immunostaining showed no difference between PLA2R and control while for WERI-Rb1 a moderate staining of cytoplasmic and membrane granular pattern was obtained. Considering CD209, MRC2 and MRC1, an important granular membrane and cytoplasmic staining was observed for both retinoblastoma cell lines. Then, expression of mannose receptors was evaluated on human retinoblastoma tumors. Rb102, Rb111 and Rb200 tissues were obtained from xenografted mouse with primary cancer cells of three patients affected by retinoblastoma (Figure 2B). Granular membrane and cytoplasmic localization of LY75, CD209, MRC2 and MRC1 were observed with different immunostaining intensities in tissues. In Rb102, tumor area LY75, CD209 and MCR2 were strongly expressed while in Rb111 tumor expression of LY75 appears higher than CD209, MRC2 or MRC1. Similarly, tumor area in Rb200 is tightly immunostained and particularly for LY75 and CD209. By these experiments we highlighted the overexpression of LY75, CD209, MRC2 and MRC1 on retinoblastoma and point out their potential interest for targeted therapy.

Protein expression was also performed by Western blot analysis. We evaluated expression of LY75, CD209, MRC2 and MRC1 in retinoblastoma cells and tissues (Figure 2C). Rabbit polyclonal antibody anti-actin was used to control the protein loading. The results obtained confirm the high expression of LY75, CD209, MRC2 and MRC1, in vitro (except that MRC2 expression is less pronounced for WERI-Rb1) and in vivo for the samples tested. However, Western blot expression profile was also performed on other human cancer cell lines (see ESI Figure S19) and a moderate expression of LY75 is found in prostate (LNCaP), breast (MDA-MB-231 and MCF-7), colon (HCT-116) and osteosarcoma (Saos-2) cancer cells. This excludes the use of LY75 as a specific target of retinoblastoma. MRC1 and CD209 proteins are particularly overexpressed in retinoblastoma compared to the other cancer cell lines. By contrast, MRC2 is also found in Saos-2 cells but not in the other cancer cells studied. Thus, CD209 and MRC1 could be specific targets for retinoblastoma as shown by Western blot analyses.

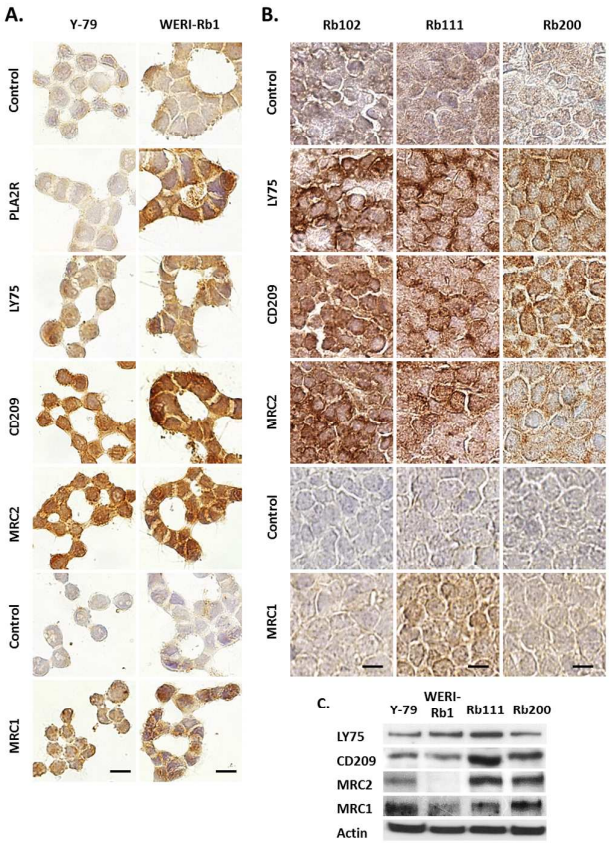

Figure 2. Protein expression of mannose receptors in cells and tissues. Immunohistochemistry analyses were performed **(A)** on human retinoblastoma cell lines (Y-79 and WERI-Rb1) and **(B)** on human retinoblastoma tissues (Rb102, Rb111 and Rb200). Scale bars: 10 µm. Western blot analysis was performed **(C)** on human retinoblastoma cells Y-79 and WERI-Rb1 and tissues, Rb111 and Rb200.

The results obtained by these different analysis methods were summarized and arbitrary semi-quantified (Table 1). The data indicate a correlation between the different analytical approaches. Indeed, CD209 and MRC2 mannose receptors are mainly overexpressed in retinoblastoma cell lines and tumors.

		PLA2R	LY75	CD209	MRC2	MRC1
Transcriptomic	Y-79*	-/+	-/+	+++	+++	*N.D.*
	WERI-Rb1*	-/+	-/+	+++	+++	*N.D.*
	Tumors (n=37)	-/+	-/+	+++	+	*N.D.*
IHC	Y79	-/+	++	+++	+++	+
	WERI-Rb1	++	++	+++	+++	+
	Rb102	*N.D.*	++	+++	+++	-/+
	Rb111	*N.D.*	+++	+++	+++	+++
	Rb200	*N.D.*	++	++	+	-/+
WB	Y-79	*N.D.*	+	++	++	+++
	WERI-Rb1	*N.D.*	++	++	-/+	+
	Rb111	*N.D.*	++	+++	+++	++
	Rb200	*N.D.*	+	+++	+++	+++

Table 1. Mannose receptors expression quantified by transcriptomic, immunohistochemistry (IHC) and Western blot (WB) analytical methods in retinoblastoma cells and tissues. N.D.; none determined. *[3].

In order to study the targeting of MRC2 and CD209 mannose receptors, MSN nanoparticles covalently grafted with commercial anti-MRC2 or/and anti-CD209 antibodies were synthesized (Figure 3). The ligation of the antibodies to the nanoparticles was performed through a specific semi-carbazide/aldehyde reaction. The semi-carbazide function was first grafted on the nanoparticles. The aldehyde function was obtained through mild oxidation of the carbohydrate chains of the Fc part of the antibodies. This strategy leads to an end-on orientation of the antibodies at the surface of the nanoparticles and thus maintains a maximal activity [25, 26]. Characterizations of nanoparticles: size, repartition, surface grafting and morphology were performed by DLS, TEM, UV-visible absorption and FTIR spectra analysis (see ESI Figure S3-S16).
The antibodies-grafted MSN were designed to improve therapeutic targeting in two-photon PDT.

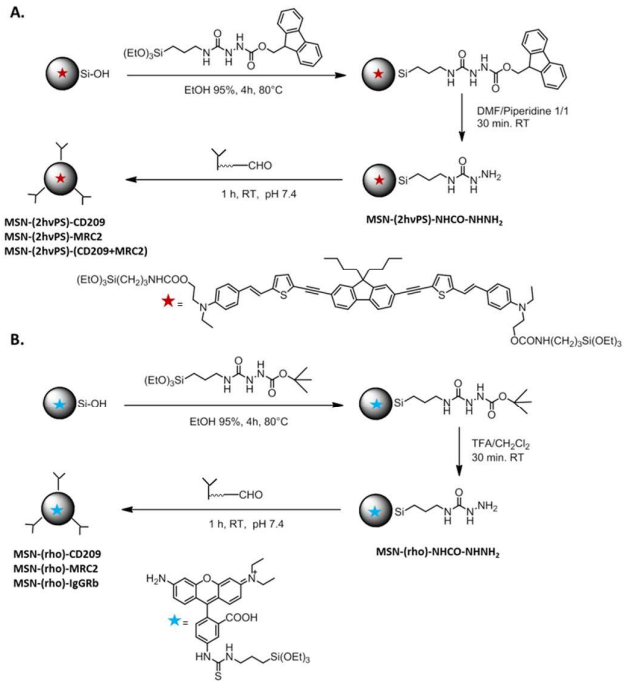

Figure 3. Synthesis of MSN loaded with rhodamine (rho) (A) or two-photon photosensitizer (2hvPS) (B) and grafted with or without anti-IgGRb, anti-CD209 or anti-MRC2 antibodies.

Firstly, confocal microscopy was performed on retinoblastoma cells using rhodamine-loaded MSN (Figure 4). The cellular uptake was assessed by fluorescence imaging on living Y-79 and WERI-Rb1 incubated 5 h with antibodies-grafted MSN-(rho)-IgGRb, MSN-(rho)-CD209, MSN-(rho)-MRC2 or the non-grafted one MSN-(rho)-NHCO-NHNH2 at 20 µg.mL-1. MSN-(rho)-IgGRb and MSN-(rho)-NHCO-NHNH2 were introduced as unspecific and untargeted controls, respectively. Cells were co-stained with a lysosomal marker. The emission of rhodamine was localized within the cells for MSN-(rho)-CD209 and MSN-(rho)-MRC2, while MSN-(rho)-IgGRb and MSN-(rho)-NHCO-NHNH2 (not shown) remain outside the cells. MSN-(rho)-CD209 and MSN-(rho)-MRC2 are co-localized with the lysosomes thus demonstrating the successful internalization through the endolysosomal pathway.

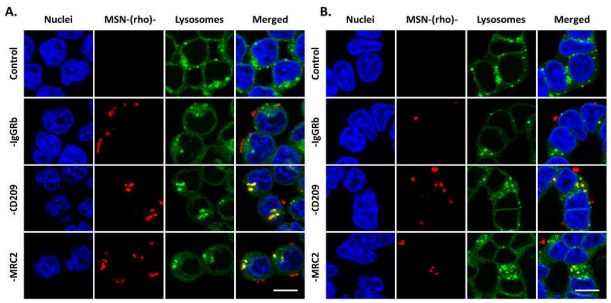

Figure 4. Confocal imaging of MSNs cellular uptake. Living (A) Y-79 cells or (B) WERI-Rb1 cells were incubated or not 5 h with MSN-(rho)- (20 µg.mL^{-1}) Nuclei were stained with Hoechst (blue) and lysosomes with Lysotracker (green) to show nanoparticles co-localization. Scale bars: 5 µm.

The MSNs loaded with the photosensitizers were then screened under two-photon excitation in retinoblastoma cells (Figure 5). Y-79 and WERI-Rb1 cells were seeded in a poly-ornithine coated 384 multi-well plate and incubated 5 h with a single-dose of 40 µg.mL-1 of MSN-(2hvPS)-NHCO-NHNH2, MSN-(2hvPS)-CD209, MSN-(2hvPS)-MRC2 or MSN-(2hvPS)-(CD209+MRC2). Irradiation was performed with a Carl Zeiss confocal microscope with a focused laser beam and at maximum laser power (laser input 3 W, laser output before the objective 900 mW.cm-2). The well was irradiated with three scans of 1.57 s each with a 10x magnification objective. The MTS assay was performed two days after irradiation. The safety of these nanoparticles without irradiation was verified following the same treatment conditions (see ESI, Figure S20). The photodynamic efficiency obtained indicates that MSN-(2hvPS)-CD209 and MSN-(2hvPS)-MRC2 were able to induce significant toxicity with around 20% to 25% of cell death for Y-79 and WERI-Rb1 cells, respectively. Cells treated with MSN-(2hvPS)-(CD209+MRC2) showed an increased toxicity with 30% of retinoblastoma cell death. In contrast, irradiated MSN-(2hvPS)-NHCO-NHNH2 did not induce any toxicity to the cells. These data provide new evidences of the potential of targeted mesoporous silica nanoparticles for retinoblastoma treatment by a non-invasive method with reduced side effects.

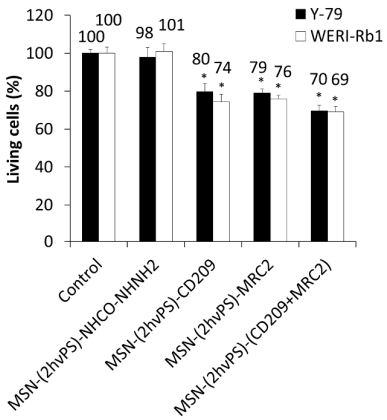

Figure 5. Two-photon PDT efficiency on retinoblastoma cell lines. Y-79 or WERI-Rb1 cells were incubated with a single dose of 40 µg.mL^{-1} of MSN-(2hvPS)-NHCO-NHNH2, MSN-(2hvPS)-CD209, MSN-(2hvPS)-MRC2 or MSN-(2hvPS)-(CD209+MRC2) for 5 h and then irradiated at 760 nm, with 3 scans of 1.57 s each. Cells were allowed to grow for 2 days and cell viability was quantified by MTS assay. * p-value<0.05 versus control (Student's t test).

The primary focus of this study was to further improve the specificity in the treatment of retinoblastoma. It was already known that some mannose receptors were involved in the active transport of nanoparticles in Y-79 retinoblastoma cells [17]. In this work, mannose receptors expressions were evaluated in immortalized cell lines and in human retinoblastoma tumors. Combining several biological analyzes, we demonstrated for the first time that CD209 and MRC2 could be specific targets for retinoblastoma. Due to their overexpression in cells and tissues, we focused on the synthesis of antibodies-grafted MSN designed for two-photon photodynamic therapy. Herein, commercial specific antibodies were grafted on MSN using an oriented strategy. The cellular uptake of these MSNs mediated by the endocytosis pathway and the co-localization into the lysosomes was successfully monitored by confocal imaging on living retinoblastoma cell lines with rhodamine-loaded MSNs and a co-localization into the lysosomes. The potential of biphotonic PDT, to control in time and space the cytotoxic effect, induced by using mannose receptors antibodies-grafted nanoparticles was also demonstrated. Using two-photon excitation in the near infra-red region exhibits strong advantages such as deeper penetration in tissues (down to 2 cm), lower scattering losses and three-dimensional spatial resolution (operative for an efficient and safe treatment of retinoblastoma). Work is in progress to provide a local administration in an orthotopic retinoblastoma mouse model newly developed at Institut Curie. In parallel, current efforts are made on downsizing the MSN diameter in order to cross the blood retinal barrier [27]. Indeed, eye drop are easy to use and ensure high levels of patient compliance and in this context, innovative formulations of nanomaterials as eye drops are promising systems for ophthalmological drug delivery.

Acknowledgements

We thank the PIC retinoblastoma program of Institut Curie allowing the development of more specific therapeutic for retinoblastoma disease, the Montpellier RIO Imaging (MRI) platform for access to the confocal microscopy and the electron and analytical department of Université de Montpellier for the access to TEM imaging. We particularly thank Drs. Isabelle Aerts, Livia Lumbroso-Le-Rouic and Nathalie Cassoux from the pediatric oncology and ophthalmology department of the hospital complex of Institut Curie and Dr Didier Decaudin from the Preclinical Investigation Laboratory of the Transfer Department of the Research Center of Institut Curie.

Experimental part

Cell culture conditions. Human retinoblastoma cancer cells (Y-79 and WERI-Rb1) were purchased from ATCC® and cultured in RPMI-1640 medium supplemented with 20% fetal calf serum (FCS), 100 IU penicillin and 100 µg.mL^{-1} streptomycin. Cells were allowed to grow in humidified atmosphere at 37 °C under 5% CO_2.

Human tumor sample processing. A total of 37 tumors from patients having received no treatment prior to enucleation were studied. Immediately following enucleation, a needle was inserted through the eye's anterior chamber to extract a tumor sample by aspiration. The tumor sample was placed in RPMI medium on ice, resuspended, and counted. This sample was then centrifuged to remove all media and snap frozen for later extraction. RNA was extracted using Qiazol (Qiagen, Courtaboeuf, France) according to manufacturer's instruction and purified using mirRNeasy Mini kit (Qiagen). The concentration, integrity and purity of each RNA sample were measured using RNA 6000 LabChip kit with the Agilent 2100 Bioanalyser (Agilent technologies, Palo Alto, CA). For DNA extraction, samples were first incubated in a lysis buffer with proteinase K, recombinant (Roche, Boulogne-Billancourt, France). They were next incubated with RNAse A (Roche).

Immunochemistry analysis. For immunocytochemical staining, Y-79 and WERI-Rb1 cells were seeded on poly-ornithine coated coverslips and fixed with a paraformaldehyde solution 20 min at room temperature (RT). Then, cells were permeabilized with 0.2% Triton X-100 (4 min, RT) and endogenous peroxidase were blocked with 1% H_2O_2 (15 min, RT). After saturation with normal horse or donkey serum (1:40 dilution, 30 min, 37°C), primary antibodies, mouse monoclonal antibody anti-MRC1 (Abnova), rabbit polyclonal antibodies anti-LY75 (Abgent), anti-CD209 (Abnova), anti-MRC2 and anti-PLA2R (Abcam) were incubated overnight at 4°C (10 µg.mL^{-1}). Normal rabbit anti-IgGRb (Dako) and mouse anti-MOPC21 (Sigma Immunochemicals) were used for negative control of unspecific staining at the same concentration. Antibodies were revealed by using secondary biotin antibodies anti-mouse or anti-rabbit (40 min, RT) followed by streptavidin-peroxidase complex (40 min, RT) and 3,3' di-aminobenzidine tetrachloride (Sigma) as a substrate. The samples were counterstained with Hematoxylin (Dako) and observed on an upright Zeiss Axioimager microscope (63x oil lens) equipped with a camera Coolsnap color and controlled by the software MetaMorph. Immunohistochemical stainings were performed on tissue sections of paraffin-embedded samples of Rb102, Rb111 and Rb200 retinoblastoma. The immunohistochemical analysis of receptors was performed on dewaxed and rehydrated slides using antibodies anti-MRC2, anti-CD209, anti-LY75 and anti-MRC1 as mentioned above. Digital slide scanner Nanozoomer-XR 12000 was used to analyze the immunostaining. Specificity validation efforts were already performed for all the antibodies following stringent processes and using a combination of several approaches and applications [17-24].

Western blots analysis. Cellular extracts were obtained after 15 min at 4°C incubation in RIPA buffer containing 50 mM, Trizma pH 8.0, 150 mM NaCl, 0.5% deoxycholic acid, 1% NP40, 10% glycerol, 0.5 mM EDTA, 0.1% SDS and Complete protease inhibitors (Roche, Switzerland). For human retinoblastoma tumor protein extractions, Rb111 and Rb200 tissues were homogenized in RIPA buffer by using an Ultra-Turrax®. Extracts were centrifuged at 10,000 g for 15 min at 4°C and proteins were quantified by Bradford assay. Constant amount of whole lysate was resolved by SDS-PAGE, transferred onto PVDF membranes by electroblotting, and probed with specific anti-mannose receptors. Anti-LY75 (Abgent) was used at 2.5 µg.mL^{-1}. Anti-CD209, anti-MRC2 and anti-MRC1 (Santa Cruz Biotechnology) were used at 1.0 µg.mL^{-1}. Rabbit polyclonal antibody anti-actin (Abcam) was used for control of protein loading. Immunoblotting was performed using mouse or rabbit secondary antibody coupled with horseradish peroxidase and revealed using the ECL detection system (Amersham).

Confocal imaging on living retinoblastoma cells. Cells were seeded onto poly-ornithine coated glass dishes (Ibidi, Biovalley, France) at a density of 10^6 cells.cm^{-2}. Twenty four hours after seeding, cells were incubated 5 h with 20 µg.mL^{-1} fluorescent loaded nanoparticles MSN-(rho)-IgGRb, MSN-(rho)-CD209 or MSN-(rho)-MRC2. Then, lysosomes were labeled with LysoTracker green DND-26 (Life Technologies, France) as described by the manufacturer and nuclei were counter-stained using Hoechst 33342 (Invitrogen, France). Before imaging, cells were washed with RPMI media and representative images were obtained under a Zeiss Axio Observer confocal microscope with a Plan-Apochromat 63x/1.40 Oil objective.

PDT and cell death measurement. For two-photon excitation, retinoblastoma cells were seeded into 384 multi-well glass bottom (thickness 0.17 mm) plates, with a black polystyrene frame, 2.10^3 cells per well in 50 µL culture medium and allowed to grow for 24 h. Cells were then incubated for 5 h with or without 40 µg.mL^{-1} of MSN-(2hvPS)-CD209, MSN-(2hvPS)-MRC2 and MSN-(2hvPS)-(CD209+MRC2). After incubation with MSN, cells were submitted or not to laser irradiation with a Carl Zeiss confocal microscope (numerical aperture 0.3, 10x magnification) with a focused laser beam at maximum laser power (input 3W, output before the objective 900 mW.cm^{-2}). Half of each well was irradiated at 760 nm by 3 scans of 1.57 s each on four different non-overlapping areas. Two days after irradiation, a MTS assay was performed to evaluate the phototoxicity of MSN as described before [17].

Statistical analysis. Statistical analysis was performed using the Student's *t* test to compare paired groups of data. A *p*-value < 0.05 was considered to be statistically significant.

Notes and references

References

1. S. De Francesco, P. Galluzzi, A. Del Longo, E. Piozzi, A. Renieri, C. Menicacci, F. Mari, F. Munier, T. Hadjistilianou and D. Mastrangelo, *Eur J Ophthalmol*, 2012, 22, 857-860.
2. D. Mastrangelo, S. De Francesco, A. Di Leonardo, L. Lentini and T. Hadjistilianou, *Med Sci Monit*, 2008, 14, RA231-240.
3. J. McEvoy, J. Flores-Otero, J. Zhang, K. Nemeth, R. Brennan, C. Bradley, F. Krafcik, C. Rodriguez-Galindo, M. Wilson, S. Xiong, G. Lozano, J. Sage, L. Fu, L. Louhibi, J. Trimarchi, A. Pani, R. Smeyne, D. Johnson and M. A. Dyer, *Cancer Cell*, 2011, 20, 260-275.
4. F. Doz, *Arch Pediatr*, 2006, 13, 1329-1337.
5. M. V. Parulekar, *Early Hum Dev*, 2010, 86, 619-625.

6. D. Clark and L. Mao, *Dis Markers*, 2012, 33, 1-10.
7. S. Griegel, M. F. Rajewsky, T. Ciesiolka and H. J. Gabius, *Anticancer Res*, 1989, 9, 723-730.
8. K. Jain, P. Kesharwani, U. Gupta and N. K. Jain, *Biomaterials*, 2012, 33, 4166-4186.
9. A. Naeem, M. Saleemuddin and R. H. Khan, *Curr Protein Pept Sci*, 2007, 8, 261-271.
10. N. C. Reichardt, M. Martin-Lomas and S. Penades, *Chem Soc Rev*, 2013, 42, 4358-4376.
11. O. Vaillant, K. El Cheikh, D. Warther, D. Brevet, M. Maynadier, E. Bouffard, F. Salgues, A. Jeanjean, P. Puche, C. Mazerolles, P. Maillard, O. Mongin, M. Blanchard-Desce, L. Raehm, X. Rebillard, J. O. Durand, M. Gary-Bobo, A. Morere and M. Garcia, *Angew Chem Int Ed Engl*, 2015, 54, 5952-5956.
12. I. Laville, S. Pigaglio, J. C. Blais, F. Doz, B. Loock, P. Maillard, D. S. Grierson and J. Blais, *J Med Chem*, 2006, 49, 2558-2567.
13. M. Lupu, C. D. Thomas, P. Maillard, B. Loock, B. Chauvin, I. Aerts, A. Croisy, E. Belloir, A. Volk and J. Mispelter, *Photodiagnosis Photodyn Ther*, 2009, 6, 214-220.
14. P. Maillard, B. Loock, D. S. Grierson, I. Laville, J. Blais, F. Doz, L. Desjardins, D. Carrez, J. L. Guerquin-Kern and A. Croisy, *Photodiagn. Photodynamic Ther.*, 2007, 4, 261-268.
15. M. Gary-Bobo, O. Vaillant, M. Maynadier, I. Basile, A. Gallud, K. El Cheikh, E. Bouffard, A. Morere, X. Rebillard, P. Puche, P. Nirde and M. Garcia, *Curr Med Chem*, 2013, 20, 1946-1955.
16. A. Gallud, A. Da Silva, M. Maynadier, I. Basile, S. Fontanel, C. Lemaire, P. Maillard, M. Blanchard-Desce, O. Mongin, A. Morere, L. Raehm, J. O. Durand, M. Garcia and M. Gary-Bobo, *Journal of Clinical and Experimental Ophthalmology*, 2013, 4, 4-8.
17. M. Gary-Bobo, Y. Mir, C. Rouxel, D. Brevet, O. Hocine, M. Maynadier, A. Gallud, A. Da Silva, O. Mongin, M. Blanchard-Desce, S. Richeter, B. Loock, P. Maillard, A. Morere, M. Garcia, L. Raehm and J. O. Durand, *Int J Pharm*, 2012, 432, 99-104.
18. P. F. McKay, N. Imami, M. Johns, D. A. Taylor-Fishwick, L. M. Sedibane, N. F. Totty, J. J. Hsuan, D. B. Palmer, A. J. George, B. M. Foxwell and M. A. Ritter, *Eur J Immunol*, 1998, 28, 4071-4083.
19. T. B. Geijtenbeek, R. Torensma, S. J. van Vliet, G. C. van Duijnhoven, G. J. Adema, Y. van Kooyk and C. G. Figdor, *Cell*, 2000, 100, 575-585.
20. S. Pohlmann, G. J. Leslie, T. G. Edwards, T. Macfarlan, J. D. Reeves, K. Hiebenthal-Millow, F. Kirchhoff, F. Baribaud and R. W. Doms, *J Virol*, 2001, 75, 10523-10526.
21. N. Ikenaga, K. Ohuchida, K. Mizumoto, S. Akagawa, K. Fujiwara, D. Eguchi, S. Kozono, T. Ohtsuka, S. Takahata and M. Tanaka, *PLoS One*, 2012, 7, e40434.
22. K. A. Maupin, A. Sinha, E. Eugster, J. Miller, J. Ross, V. Paulino, V. G. Keshamouni, N. Tran, M. Berens, C. Webb and B. B. Haab, *PLoS One*, 2010, 5, e13002.
23. Y. Hirata, M. Tabata, H. Kurobe, T. Motoki, M. Akaike, C. Nishio, M. Higashida, H. Mikasa, Y. Nakaya, S. Takanashi, T. Igarashi, T. Kitagawa and M. Sata, *J Am Coll Cardiol*, 2011, 58, 248-255.
24. P. Y. Zhuang, M. J. Zhu, J. D. Wang, X. P. Zhou, Z. W. Quan and J. Shen, *J Dig Dis*, 2013, 14, 45-50.
25. J. M. Montenegro, V. Grazu, A. Sukhanova, S. Agarwal, J. M. de la Fuente, I. Nabiev, A. Greiner and W. J. Parak, *Adv Drug Deliv Rev*, 2013, 65, 677-688.
26. E. Secret, K. Smith, V. Dubljevic, E. Moore, P. Macardle, B. Delalat, M. L. Rogers, T. G. Johns, J. O. Durand, F. Cunin and N. H. Voelcker, *Adv Healthc Mater*, 2013, 2, 718-727.
27. D. Warther, C. Mauriello Jimenez, L. Raehm, C. Gerardin, J. O. Durand, K. El Cheikh, A. Gallud, A. Morère, M. Gary-Bobo, M. Maynadier and M. Garcia, *RSC Advances*, 2014, DOI: 10.1039/c4ra05310a.